MBP 5-10, 1161

Reduction of Eddy Current Loss in Rectangular Coils Using Magnetic Shield: Analysis with Homogenization Method

Shogo Fujita[1,2], and Hajime Igarashi[1], *Member, IEEE*

[1] Graduate School of Informatics Science and Technology, Hokkaido University, Sapporo, 060-0184
[2] Research Fellow of Japan Society for the Promotion of Science, Tokyo, 102-0083, Japan
fujita@em.ist.hokudai.ac.jp

Rectangular coils have been widely used in rotating machines and transformers because of high space factor and low DC resistance. However, eddy current losses due to skin and proximity effects in the rectangular coils cannot be ignored especially when carrier harmonic increases. The eddy current loss due to the proximity effect would be effectively reduced by shielding the coils with magnetic thin layer. In this paper, a method for homogenization-based analysis of a magnetically shielded rectangular coil is proposed. It is shown by the proposed method that the AC-resistance of a motor winding can be effectively reduced by introducing the magnetic shield.

Index Terms— **Rectangular coil, magnetic shield, homogenization method, proximity effect, complex permeability.**

I. Introduction

Recently, rectangular coils with relatively large cross-sectional area have widely been used for electric machines and devices because of its high space factor and low DC resistance [1]. On the other hand, the eddy current loss in a rectangular coil becomes significant when the carrier harmonic increases. The AC resistance coming from the eddy currents in a rectangular coil has been estimated using the resistance factor [e.g. 2]. In order to reduce the eddy current loss due to the proximity effect in a rectangular coil, magnetically shielded wire would be effective, as is the case for round wires [3]. However, it would be difficult to consider the effect of the magnetic shield using this analytical method. Analysis of the eddy current loss using conventional finite element method (FEM) would require fairly fine discretization of the coil region because fine elements have to be smaller than the skin depth.

For the analysis of magnetically shielded round coils, the authors have proposed a semi-analytical homogenization method using the macroscopic permeability [4-7]. In this paper, a homogenization method to analyze electric apparatus using a magnetically shielded rectangular coil is proposed. In the proposed method, which is an extension of the method for a shielded round coil [5, 6], the coil region is modeled by a uniform material with the macroscopic permeability of a tensor form considering the anisotropy coming from the rectangular shape. The rectangular coil is approximated by an elliptic coil to express the macroscopic permeability in a closed form. The proposed method allows us to perform the field analysis of electric apparatus using a shielded rectangular coil with a reduced computing cost. Using this method, we evaluate how much the AC resistance can be reduced by introducing the shielding to the rectangular windings of electric motors.

II. Complex Permeability of Magnetic Shield

The magnetic shielding layer is here approximated by a slab assuming that the layer is sufficiently thin. Under this approximation, the complex permeability of the shielding layer is given by [9, 10]

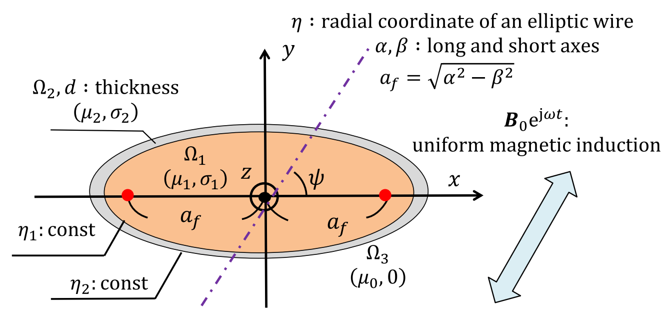

Fig.1 Magnetically shielded wire (MSW) with elliptic cross section immersed in time-harmonic magnetic induction $\boldsymbol{B}_0 \mathrm{e}^{\mathrm{j}\omega t}$.

$$\dot{\mu}_r^{\mathrm{slab}} = \mu_r \frac{\tan\zeta}{\zeta}, \zeta \coloneqq \frac{d}{2\delta_2}(1-\mathrm{j}) \tag{1}$$

where $\delta_2 \coloneqq \sqrt{2/(\omega\mu_2\sigma_2)}$ denotes the skin depth of the shielding layer (see Fig.1). It is now unnecessary to subdivide the shielding layer into finite element smaller than the skin depth because the eddy current effects have been already included in (1).

III. Complex Permeability of Shielded Elliptic Coil

The approach for the shielded round coil presented in [5, 6] is here extended to the shielded rectangular coil. The rectangular coil is here approximated with an elliptic coil to make an analytic evaluation of the macroscopic permeability. Let us consider an elliptic wire immersed in time-harmonic magnetic induction $\boldsymbol{B}_0 \mathrm{e}^{\mathrm{j}\omega t}$ as shown in Fig.1. To analyze the electromagnetic field, we introduce the elliptic coordinates (η, ψ, z) [7, 10] defined by

$$\left(\frac{x}{a_f \cosh\eta}\right)^2 + \left(\frac{y}{a_f \sinh\eta}\right)^2 = 1, \tag{2a}$$

$$\left(\frac{x}{a_f \cos\psi}\right)^2 - \left(\frac{y}{a_f \sin\psi}\right)^2 = 1\,. \tag{2b}$$

The Maxwell equations under the quasi-static approximation can be reduced to the Helmholtz equation expressed in the elliptic coordinate as

$$\frac{1}{a_f^2(\cosh^2\eta - \cos^2\psi)}\frac{\partial^2 E_z}{\partial \eta^2} + \frac{1}{a_f^2(\cosh^2\eta - \cos^2\psi)}\frac{\partial^2 E_z}{\partial \psi^2} + k^2 E_z = 0\,, \quad (3a)$$

$$H_\psi = -\frac{\mathrm{j}}{\omega\mu}\frac{\partial E_z}{\partial \eta}. \quad (3b)$$

where $k \coloneqq \sqrt{-\mathrm{j}\omega\mu_1\sigma_1} = (1-\mathrm{j})/\delta_1\,, \delta_1 \coloneqq \sqrt{2/(\omega\mu_1\sigma_1)}$. Equation (3a) can be analytically solved using the variable separation.

The magnetic-conductive shield Ω_2 can be regarded as an insulated layer with the complex permeability $\dot{\mu}_2^{\mathrm{slab}}$. By imposing the tangential continuity of electromagnetic fields on $\Omega_1 - \Omega_2$ and $\Omega_2 - \Omega_3$ interfaces, we obtain a system of equations of the form

$$\begin{bmatrix} \mathrm{se}_1(\mathrm{j}\eta_1, q) & -1/\mathrm{e}^{\eta_1} & -\mathrm{e}^{\eta_1} & 0 \\ \nu_1 \mathrm{se}_1'(\mathrm{j}\eta_1, q) & 1/\mathrm{e}^{\eta_1} & -\mathrm{e}^{\eta_1} & 0 \\ 0 & 1 & \mathrm{e}^{2\eta_2} & -1 \\ 0 & -\nu_2 & \nu_2\mathrm{e}^{2\eta_2} & 1 \end{bmatrix}\begin{bmatrix} c_1^x \\ c_2^x \\ c_3^x \\ c_4^x \end{bmatrix} = -\mathrm{j}\omega\mathrm{e}^{2\eta_2}B_0^x\begin{bmatrix} 0 \\ 0 \\ 1 \\ 1 \end{bmatrix}, \quad (4a)$$

$$\begin{bmatrix} \mathrm{ce}_1(\mathrm{j}\eta_1, q) & -1/\mathrm{e}^{\eta_1} & -\mathrm{e}^{\eta_1} & 0 \\ \nu_1 \mathrm{ce}_1'(\mathrm{j}\eta_1, q) & 1/\mathrm{e}^{\eta_1} & -\mathrm{e}^{\eta_1} & 0 \\ 0 & 1 & \mathrm{e}^{2\eta_2} & -1 \\ 0 & -\nu_2 & \nu_2\mathrm{e}^{2\eta_2} & 1 \end{bmatrix}\begin{bmatrix} c_1^y \\ c_2^y \\ c_3^y \\ c_4^y \end{bmatrix} = \mathrm{j}\omega\mathrm{e}^{2\eta_2}B_0^y\begin{bmatrix} 0 \\ 0 \\ 1 \\ 1 \end{bmatrix}, \quad (4b)$$

where $\nu_1 = \dot{\mu}_2(\omega)/\mu_1\,, \nu_2 = \mu_0/\dot{\mu}_2(\omega)\,, q = \left(k a_f\right)^2/4 \in \mathbb{C}$, and $\mathrm{se}_1(\mathrm{j}\eta, q)$, $\mathrm{ce}_1(\mathrm{j}\eta, q)$ denote the first order Mathieu functions [10-12], and the prime denotes the derivative with respect to the argument η. Here the coefficient c_4^x, c_4^y are relevant to the dipole fields induced by the proximity effect.

By solving (4), we can obtain the frequency-dependent magnetization of the magnetically-shielded elliptic coil as

$$\boldsymbol{M} = \frac{\mathrm{e}^{2\eta_1}}{(\alpha+d)(\beta+d)}\frac{1}{\mu_0}\left(-B_0^x\dot{\gamma}_x\mathbf{e}_x + B_0^y\dot{\gamma}_y\mathbf{e}_y\right), \quad (5a)$$

$$\dot{\gamma}_x = \frac{\lambda_1\dfrac{\mathrm{se}_1(\mathrm{j}\eta_1,q)}{\nu_1\mathrm{se}_1'(\mathrm{j}\eta_1,q)} + \lambda_2}{\lambda_3\dfrac{\mathrm{se}_1(\mathrm{j}\eta_1,q)}{\nu_1\mathrm{se}_1'(\mathrm{j}\eta_1,q)} + \lambda_4}, \quad (5b)$$

$$\dot{\gamma}_y = \frac{\lambda_1\dfrac{\mathrm{ce}_1(\mathrm{j}\eta_1,q)}{\nu_1\mathrm{ce}_1'(\mathrm{j}\eta_1,q)} + \lambda_2}{\lambda_3\dfrac{\mathrm{ce}_1(\mathrm{j}\eta_1,q)}{\nu_1\mathrm{ce}_1'(\mathrm{j}\eta_1,q)} + \lambda_4} \quad (5c)$$

where $\lambda_1 = -h_1\nu_2 - h_2,\ \lambda_2 = h_2\nu_2 + h_1\,, \lambda_3 = h_1\nu_2 - h_2, \lambda_4 = -h_2\nu_2 + h_1, h_1 = \mathrm{e}^{2\eta_1} - \mathrm{e}^{2\eta_2}, h_2 = \mathrm{e}^{2\eta_1} + \mathrm{e}^{2\eta_2}$. From (4), we can derive the complex permeability as [6]

$$\dot{\mu}_r^x = \frac{\cosh\eta_1}{\sinh\eta_1}\frac{1+\dfrac{\mathrm{e}^{2\eta_2}}{\mathrm{e}^{2\eta_1}}\dot{\gamma}_x}{1-\dfrac{\mathrm{e}^{2\eta_2}}{\mathrm{e}^{2\eta_1}}\dot{\gamma}_x}, \dot{\mu}_r^y = \frac{\sinh\eta_1}{\cosh\eta_1}\frac{1+\dfrac{\mathrm{e}^{2\eta_2}}{\mathrm{e}^{2\eta_1}}\dot{\gamma}_y}{1-\dfrac{\mathrm{e}^{2\eta_2}}{\mathrm{e}^{2\eta_1}}\dot{\gamma}_y}. \quad (6a, b)$$

The homogenized magnetic permeability of a multi-turn elliptic coil can be evaluated from the extended Ollendorff formula [7, 13] given by

$$\langle\dot{\mu}_r^x(\omega)\rangle = 1 + \frac{f_v(\dot{\mu}_r^x(\omega)-1)}{1+N_x(1-f_v)(\dot{\mu}_r^x(\omega)-1)}, \quad (7a)$$

$$\left\langle\dot{\mu}_r^y(\omega)\right\rangle = 1 + \frac{f_v\left(\dot{\mu}_r^y(\omega)-1\right)}{1+N_y(1-f_v)\left(\dot{\mu}_r^y(\omega)-1\right)}, \quad (7b)$$

where N_x, N_y, f_v denote the diamagnetic constants and volume fraction, respectively. The homogenization method using the complex permeability and (7), on which the present method is based, has been experimentally validated in [6]. Using (7), the multi-turn coil can be treated as a uniform material which has the tensor macroscopic permeability $[\langle\dot{\mu}_r(\omega)\rangle]$ which represents the proximity effect.

The total power $\dot{P}$ can be evaluated from the energy conservation law

$$\dot{P} = \frac{\mathrm{j}\omega}{2}\int_\Omega \mu|\boldsymbol{H}|^2\mathrm{d}v + Z_{\mathrm{skin}}|I|^2 + \mathrm{j}\omega\dot{\mu}_r^{\mathrm{slab}}\mu_0 l\pi\frac{a_f}{2}\left(\frac{1}{\mathrm{e}^{\eta_1}} - \frac{1}{\mathrm{e}^{\eta_2}}\right)\left|\frac{I}{2\pi}\right|^2, \quad (8a)$$

$$Z_{\mathrm{skin}} \coloneqq -2\cosh\eta_1\sinh\eta_1\frac{q\,\mathrm{ce}_0(\mathrm{j}\eta_1,q)}{\mathrm{ce}_0'(\mathrm{j}\eta_1,q)}R_0, \quad (8b)$$

where l is the coil length, and $\mathrm{ce}_0(\mathrm{j}\eta, q)$ denote the zeroth order Mathieu function [10-12]. The first term in (8a) represents the eddy current loss due to the proximity effect and time variation in the stored magnetic energy in air region, while the second term using (8b) represents the eddy current loss due to the skin effect. The magnetic energy stored in the magnetic shield is expressed in the third term [7, 14]. The DC resistance, R_0, in (8b) is evaluated from that of the rectangular coil. When we consider the voltage input problem, the total current I is determined by solving the FE equation coupled with the circuit equation.

IV. Numerical results

A. *Frequency characteristics of complex permeability*

In order to test the validity of the proposed approach, we compare the tensor complex permeability of the magnetically elliptical coil, whose specification is in Table I, computed by proposed method with that obtained by the unit-cell approach [15] in which the cross-section of the coil is subdivided into unit cells with the spatial periodicity, and electromagnetic field in the unit cell is computed under appropriate boundary conditions. The thickness of the shield is set to 10.0 μm. Based on the energy conservation, the macroscopic complex permeability is evaluated using the unit-cell method as [15]

$$\langle \dot{\mu}_r(\omega) \rangle = \frac{\mathrm{j}\omega \int_\Omega \frac{|\boldsymbol{B}_0|^2}{\mu_0} \mathrm{d}\Omega}{\int_{\Omega_1} \sigma |\boldsymbol{E}|^2 \mathrm{d}\Omega_1 + \mathrm{j}\omega \int_\Omega \frac{|\boldsymbol{B}|^2}{\mu} \mathrm{d}\Omega}. \quad (9)$$

The complex permeabilities computed by (7) and (9) are plotted in Fig.2, where the abscissa is the long axis α normalized by the skin depth δ_1. From Fig.2, it can be seen that the overall tendencies are in agreement while there are small discrepancies.

Next, we verify the approximation that the rectangular coil is modeled by the elliptic coil. The longer and shorter edge length of the rectangular coil are assumed to be the long and short axis of the ellipsoid, 2α and 2β, respectively. Those complex permeabilities are plotted in Fig.3. The macroscopic permeability of the rectangular coil is computed from the unit-cell method based on FEM. It can be found that the coincidence between them is satisfactory. It is remarked that it becomes difficult to compute the macroscopic permeability of the shielded coils using the unit-cell method due to small skin depth when the relative permeability of the shielding layer is larger than, say, 100. On the other hand, the proposed method can treat any shielding coils.

TABLE I
SPECIFICATION OF MAGNETIC SHIELDED WIRE WITH LOW PERMEABILITY

α [mm]	0.25	μ_{1r}	1	σ_1 [S/m]	5.76×10^7
β [mm]	0.10	μ_{2r}	10	σ_2 [S/m]	1.03×10^4

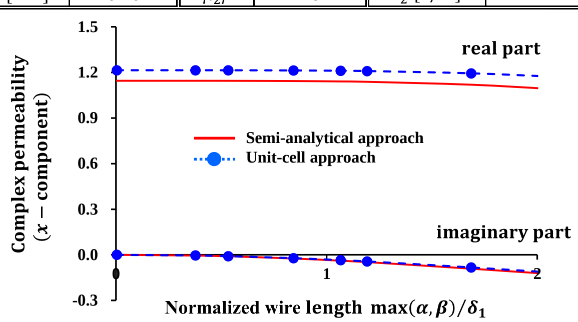

(a) $\langle \dot{\mu}_r^x \rangle$ (x-component)

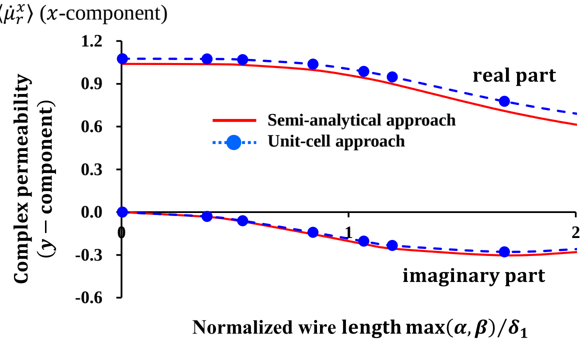

(b) $\langle \dot{\mu}_r^y \rangle$ (y-component)

Fig.2 Profiles of macroscopic complex permeability of an MSW with elliptic cross section for setting in Table I.
Abscissa denotes the ratio of long axis α to δ_1

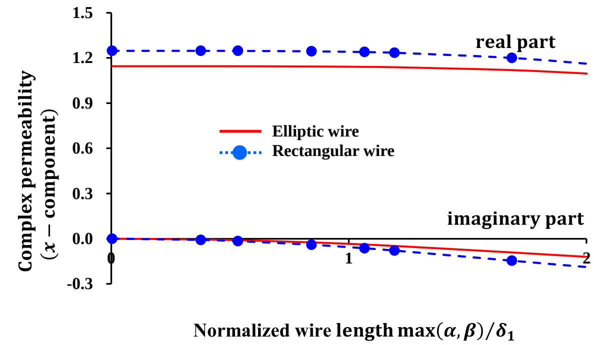

(a) $\langle \dot{\mu}_r^x \rangle$ (x-component)

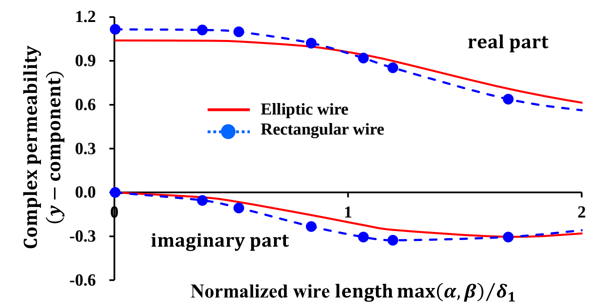

(b) $\langle \dot{\mu}_r^y \rangle$ (y-component)

Fig.3 Comparison of complex permeability of an MSW with elliptic cross section with that with rectangular cross section.

B. Impedance of magnetically shielded rectangular coil

For the numerical validation of the proposed method, we analyze the shielded rectangular coil shown in Fig.4 by the proposed method and conventional FEM. The coil specification is summarized in Table I. We assume rather low permeability for the magnetic shield to make the conventional FE analysis possible, while the proposed method is valid for higher permeabilities. The thickness of the shield is set to 20.0 μm. There are 402 and 431,976 elements in the coil region for the former and latter analyses, respectively. In Fig.4, the coil impedance Z is plotted against the normalized wire focus a_f/δ_1 for frequency ranging from 1 Hz to 300 kHz. It is found that there are no significant discrepancies in both the real and imaginary parts of Z computed by the proposed method and conventional FEM.

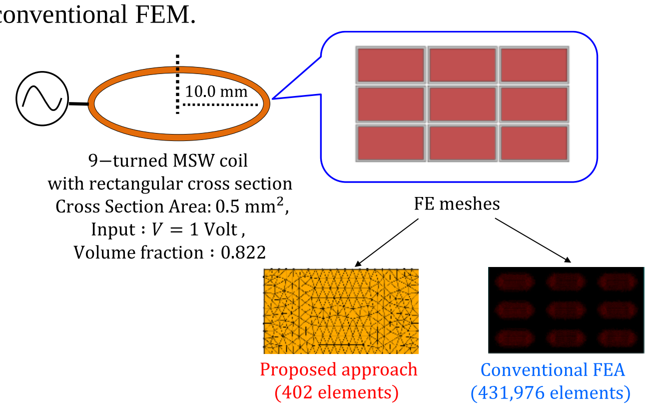

Fig. 4 Magnetically shielded rectangular coil.
In proposed method, the coil region is discretized to coarse elements with the tensor macroscopic complex permeability obtained by (7).

C. Reduction of AC resistance by magnetic shield

Using the proposed homogenization method, we analyze the AC resistance of shielded and non-shielded rectangular coils.

To do so, we consider a simple tooth model of an electric motor shown in Fig. 6. The coil specification is summarized in Table II and the shield thickness is set 10.0 μm. The AC resistance that is the real part of Z is plotted in Fig.7. We can find that AC resistance can be effectively reduced by introducing the magnetic shielding on the surface of the rectangular coil.

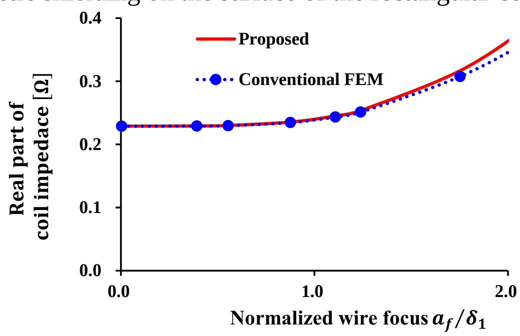

(a) real part

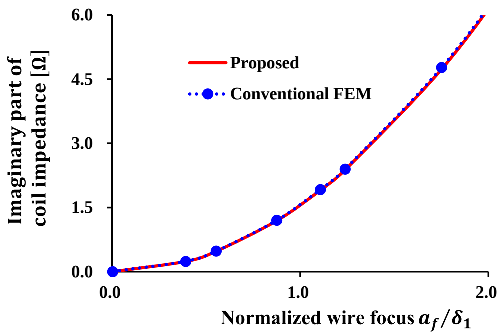

(b) imaginary part

Fig. 5 Impedance of shielded rectangular coil shown in Fig.4.
Abscissa denotes the ratio of the wire focus a_f to δ_1

TABLE II
SPECIFICATION OF MAGNETIC SHIELDED WIRE WITH LOW PERMEABILITY

α [mm]	0.9	μ_{1r}	1	σ_1 [S/m]	5.76×10^7
β [mm]	0.3	μ_{2r}	100	σ_2 [S/m]	1.03×10^7

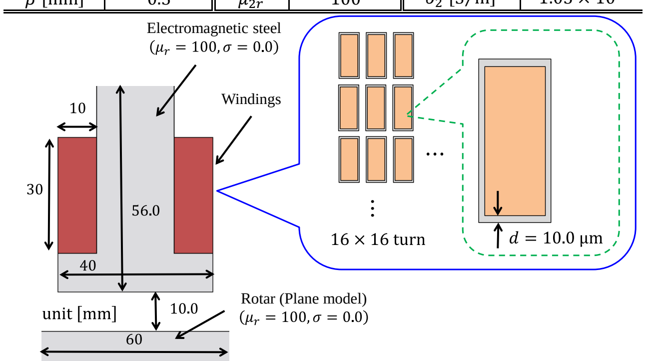

Fig. 6 Cross section of pseudo IPMSM.
In this analysis, the shape of IPMSM is approximated as a plane model.

V. CONCLUSION

A homogenization-based FEM for the analysis of magnetically shielded rectangular coil has been proposed. The macroscopic permeability of this coil is analytically expressed in a tensor form assuming that the rectangular coil is approximated with the elliptic coil. The impedance of a magnetically shielded rectangular coil computed by the proposed method has been shown to be in good agreement with that obtained by the conventional FEM. The proposed method is especially effective for analysis of 3D models with a magnetic shield of high permeability. It has been shown that the introduction of magnetic shield to the windings in an electric motor effectively reduces the AC resistance. The effect of hysteresis loss in the shielding layer will be studied in future.

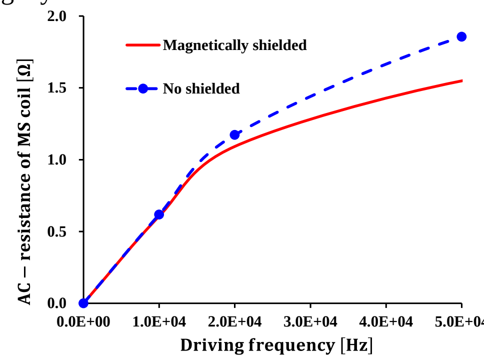

Fig. 7 Dependence of the AC resistance of MS coil of the teeth on frequency.

ACKNOWLEDGMENT

This work was supported in part by JSPS KAKENHI Grant Number 18J10778.

REFERENCES

[1] Juha Pyrhönen, Tapani Jokinen, Valéria Hrabovcová, "Design of Rotating Electrical Machines", WILEY, second ed., 2013.

[2] J. Pyrhönen, T. Jokinen, V. Hrabovcova, "Design of rotating electrical machines, 2nd ed.", Wiely, 2014.

[3] T. Mizuno, et. al., "Reduction of proximity effect in coil using magnetoplated wire", *IEEE Trans. Magn*., vol. 43, no. 6, 2003, pp. 539–548.

[4] H. Igarashi, "Semi-Analytical Approach for Finite Element Analysis of Multi-turn Coil Considering Skin and Proximity Effects", *IEEE Trans., Magn.* vol.53, no. 1, 7400107, 2017.

[5] S. Fujita, H. Igarashi, "Finite element analysis of multi - turn magnetoplated coils using homogenization method", Wiley Online Library, DOI.org/10.1002/eej.23156, 2018.

[6] S. Fujita, H. Igarashi, "Finite Element Analysis of Magnetically Shielded Wire Coils Using Homogenization Method", presented at COMPUMAG2017, *IEEE, Trans. Magn,* DOI: 10.1109/TMAG.2017.278445.

[7] S. Fujita, H. Igarashi, "Homogenization of Multi-turn Coil with Elliptic Cross Section Using Complex Permeability", submitted to COMPEL, 2018.

[8] L. Krähenbühl, D. Muller, "Thin layers in electrical engineering.Examples of shell mod-els in analyzing eddy-currents by boundary and finite element methods", *IEEE Trans. Magn*., vol. 29, no. 2, 1993, pp. 1450–1455.

[9] I. D. Mayergoyz and G. Bedrosian, "On calculation of 3-D eddy currents in conducting and magnetic shells", *IEEE Trans. Magn*., vol. 31, no. 3, 1995, pp. 1319–1324.

[10] P. Moon, D.E. Spencer, "Field theory handbook", 2nd ed., Springer-Verlag Berlin Heidelberg, 1988.

[11] Dr. Julio C. Gutiérrez-Vega, "Theory and numerical analysis of the Mathieu functions v.2.1", Monterrey, Nuevo-León, México,2008, May.

[12] N.W.McLachlan, "Theory and Application of Mathieu Functions", DOVER PUBLICATIONS, INC. NEW YORK, 1954.

[13] F. Ollendorff, "Magnetostatik der Massekerne", Arch. f. Eledtrotechnik., 25, 1931, pp. 436-447.

[14] J. A. Ferreira, "Improved analytical modeling of conductive losses in magnetic components", IEEE Trans. Power Electronics, vol. 9, no.1, 1994, pp. 127-131

[15] A. Podoltsev and B. Lebedev, "Analysis of effective resistance and eddy current losses in multiturn winding of high-frequency magnetic components", *IEEE Trans. Magn*., vol. 39, no. 1, , 2003, pp. 539–548.